MOLECULAR AND CELLULAR BIOLOGY, Dec. 2008, p. 7263–7273 Vol. 28, No. 24
0270-7306/08/$08.00+0 doi:10.1128/MCB.00313-08

Anchorage-Independent Growth of Pocket Protein-Deficient Murine Fibroblasts Requires Bypass of G_2 Arrest and Can Be Accomplished by Expression of TBX2▽†

Tinke L. Vormer, Floris Foijer,‡ Camiel L. C. Wielders, and Hein te Riele*

Division of Molecular Biology, The Netherlands Cancer Institute, Amsterdam, The Netherlands

Received 25 February 2008/Returned for modification 8 April 2008/Accepted 8 October 2008

Mouse embryonic fibroblasts (MEFs) deficient for pocket proteins (i.e., pRB/p107-, pRB/p130-, or pRB/p107/p130-deficient MEFs) have lost proper G_1 control and are refractory to Ras^{V12}-induced senescence. However, pocket protein-deficient MEFs expressing Ras^{V12} were unable to exhibit anchorage-independent growth or to form tumors in nude mice. We show that depending on the level of pocket proteins, loss of adhesion induces G_1 and G_2 arrest, which could be alleviated by overexpression of the *TBX2* oncogene. *TBX2*-induced transformation occurred only in the absence of pocket proteins and could be attributed to downregulation of the $p53/p21^{CIP1}$ pathway. Our results show that a balance between the pocket protein and p53 pathways determines the level of transformation of MEFs by regulating cyclin-dependent kinase activities. Since transformation of human fibroblasts also requires ablation of both pathways, our results imply that the mechanisms underlying transformation of human and mouse cells are not as different as previously claimed.

Deregulation of the pRB tumor suppressor pathway is a frequent event in the development of cancer (18, 31). pRB and its close homologs p107 and p130 comprise the family of so-called pocket proteins and are widely known for their role in cell cycle regulation, especially during G_1 phase. In their active, hypophosphorylated form, pocket proteins restrict cell cycle progression by binding to E2F transcription factors. E2F-pocket protein complex formation inhibits the expression of E2F target genes both by blocking E2F's ability to induce transcription and by active repression. As a result, initiation of S phase is inhibited. Upon cell cycle stimulation, cyclin D-CDK4/6 (cyclin-dependent kinase 4 or 6) and cyclin E-CDK2 complexes are activated and hyperphosphorylate the pocket proteins, resulting in liberation and activation of E2F transcription factors and initiation of S phase. Further cell cycle progression requires cyclin A-CDK1/2 activity in S phase and cyclin A-CDK1/2 and cyclin B1-CDK1 activities in G_2/M phase. The activity of cyclin-CDK complexes can be inhibited by the INK4a (inhibitor of cyclin-dependent kinase 4a) and the CIP/KIP families of CDK inhibitors (reviewed in reference 2).

Consistent with a role for pocket proteins in G_1 control, we and others have shown that complete ablation of pocket proteins in mouse embryonic fibroblasts (MEFs) abrogated G_1 arrest in response to growth-inhibitory signals, such as cell-cell contact, growth factor depletion, and DNA damage. Additionally, upon prolonged culturing or expression of constitutively active Ras (Ras^{V12}), wild-type MEFs arrested in G_1 and displayed hallmarks of senescence, while MEFs deficient for both pRb and p107 or both pRb and p130 (double-knockout [DKO] MEFs) or all three pocket proteins (triple-knockout [TKO] MEFs) were refractory to replicative and Ras^{V12}-induced senescence (6, 7, 32, 38). Similar to ablation of pocket proteins, ablation of the tumor suppressor p53 or its upstream regulator $p19^{ARF}$ also bypassed replicative and Ras^{V12}-induced senescence in MEFs (22). However, while p53- or $p19^{ARF}$-deficient MEFs could easily be transformed by Ras^{V12}, pocket protein-deficient MEFs expressing Ras^{V12} were unable to exhibit anchorage-independent growth and did not form tumors in nude mice (32; this communication). This demonstrates that the loss of pocket proteins in primary MEFs is not sufficient for Ras^{V12}-induced transformation.

In the present study, we performed a cDNA screen aimed at identifying oncogenes that collaborate with the loss of pocket proteins and Ras^{V12} in transformation of MEFs. We identified the oncogene *TBX2* as a cooperating factor in transformation of pocket protein-deficient MEFs. *TBX2* downregulates the $p53/p21^{CIP1}$ pathway both in wild-type and pocket protein-deficient MEFs, and indeed, downregulating the $p53/p21^{CIP1}$ pathway by RNA interference transformed pocket protein-deficient MEFs. In contrast to previous reports, our results demonstrate that Ras^{V12}-induced transformation of murine fibroblasts requires downregulation of both the pocket protein and p53 pathways. Since downregulation of both pathways is also required for transformation of human fibroblasts (3, 35, 46), our results indicate that the mechanisms underlying Ras^{V12}-induced transformation of human and mouse fibroblasts are not fundamentally different. Furthermore, we show that anchorage-independent growth not only requires bypass of G_1 control but also requires bypass of G_2 control.

MATERIALS AND METHODS

MEF isolation, cell culture, and retroviral infections. *$Rb^{-/-}$*, *$p107^{-/-}$*, *$p130^{-/-}$*, *$p107^{-/-}$ $p130^{-/-}$*, *$Rb^{-/-}$ $p107^{-/-}$*, *$Rb^{-/-}$ $p130^{-/-}$*, and *$Rb^{-/-}$ $p107^{-/-}$*

* Corresponding author. Mailing address: Division of Molecular Biology, The Netherlands Cancer Institute, Plesmanlaan 121, 1066 CX Amsterdam, The Netherlands. Phone: 31-20-512 20 84. Fax: 31-20-669 13 83. E-mail: h.t.riele@nki.nl.

† Supplemental material for this article may be found at http://mcb.asm.org/.

‡ Present address: Department of Systems Biology, Harvard Medical School, Boston, MA.

▽ Published ahead of print on 20 October 2008.

p130$^{-/-}$ MEFs were isolated from chimeric embryos, which were generated by injection of mutant embryonic stem cells into blastocysts as previously described (7). MEFs were cultured in Glasgow minimal essential medium (GMEM) (Invitrogen/Gibco) containing 10% fetal calf serum, 1 mM nonessential amino acids (Invitrogen/Gibco), 10 mM sodium pyruvate (Invitrogen/Gibco), 100 units of penicillin/ml (Invitrogen/Gibco), 100 μg streptomycin/ml (Invitrogen/Gibco), and 0.1 mM β-mercaptoethanol and incubated at 37°C in the presence of 5% CO_2. Retroviral supernatants were produced by calcium phosphate transfection (Invitrogen) of phoenix cells with 16 μg of the desired construct and 4 μg pCL-eco. Forty-eight hours posttransfection, retroviral supernatant was filtered using 0.45-μm filters (mixed cellulose ester membrane; Millipore) and immediately frozen using a dry ice-ethanol bath and stored at −80°C. After viral supernatant was harvested, phoenix cells were supplemented with GMEM containing medium supplements as described above, and supernatant was again harvested using the same procedure, with an interval of at least 7 h. MEFs were twice infected with viral supernatant, supplemented with Polybrene to a concentration of 4 μg/ml, during a time span of at least 7 h per infection. For serial infections, MEFs were cultured in non-virus-containing medium for 48 h between infections and reseeded before infection to obtain optimal cell density. After the last infection, MEFs were cultured in non-virus-containing medium for at least 48 h.

Constructs. The pEYK-MCF7 library and pEYK-GFP were a gift of G. Q. Daley. pCl-Eco was kindly provided by D. Peeper. pBABE-Ras^{V12} was kindly provided by T. Brummelkamp, pRetroSuper-p53 and pRetroSuper-p16^{INK4A} by A. Dirac, and pBABE-p21^{CIP1} by J. Dannenberg. The pRetroSuper-p21strong vector was previously generated and contains the following 19-mer p21^{CIP} targeting sequence: GCCCTCACTCTGTGTGTCT (11). The 19-mer p21^{CIP} targeting sequence in pRetroSuper-p21weak is ACAGGAGCAAAGTGTGCCG. The pRISC-p16^{INK4A}/p19^{ARF} vector was a gift of S. Huang; this vector is a variant of pRetroSuper (pRS) containing an additional chloramphenicol resistance marker under the control of a *TET* promoter and contains the following targeting sequence: ATCAAGACATCGTGCGATA.

Soft agar and methylcellulose assays. For soft agar assays, 6×10^4 MEFs were suspended in 2 ml of a 37°C, 0.35% soft agar solution (low gelling agarose type VII from Sigma) in GMEM containing 10% fetal calf serum, the same medium supplements as mentioned above plus gentamicin to a concentration of 0.02 mg/ml (Invitrogen/Gibco) and plated in one well of a six-well plate. To prevent cells from attaching to the bottom of the well, the 0.35% soft agar solution was poured into an ultra-low-attachment surface plate (catalog no. 3471; Corning Incorporated) coated with a 1% soft agar layer. To allow solidification of the agar, plates were incubated at 4°C for 30 min. Subsequently, cells were incubated at 37°C in the presence of 5% CO_2 for 2 to 4 weeks. A few drops of fresh medium were added twice a week. Pictures were taken using a non-phase-contrast lens (×2.5 magnification) and assembled using Axiovision 4.5. Detail images were taken using a phase-contrast lens (×5 magnification). For methylcellulose assays, 3×10^5 MEFs were suspended in 4 ml of a 37°C, 1.3% methylcellulose solution in GMEM supplemented with fetal calf serum to a concentration of 5%, penicillin to a concentration of 100 units/ml (Invitrogen/Gibco), streptomycin to a concentration of 100 μg/ml (Invitrogen/Gibco), and gentamicin to a concentration of 0.02 mg/ml (Invitrogen/Gibco) and plated in one well of a six-well ultra-low-attachment surface plate (catalog no. 3471; Corning Incorporated). A 2.6% methylcellulose stock solution was obtained from Stem Cell Technologies (catalog no. H4100). Cells were harvested by suspending 4 ml of methylcellulose culture with 40 ml ice-cold phosphate-buffered saline (PBS) (Invitrogen/Gibco), followed by centrifugation and aspiration of methylcellulose-PBS.

Recovery of retroviral integrations from soft agar colonies. Soft agar colonies were isolated using sterilized glass pipettes and propagated under attached conditions. Cells were lysed overnight (O/N) at 55°C in lysis mix containing 0.1 M Tris HCl (pH 8.5), 5 mM EDTA, 0.2 M NaCl, 0.2% sodium dodecyl sulfate (SDS), and 100 μg/ml proteinase K. Genomic DNA was isolated by phenol-chloroform-isoamyl alcohol extraction, precipitated using isopropanol, and dissolved O/N at 37°C in 10 mM Tris HCl (pH 8.0)–0.1 mM EDTA. Recovery of retroviral inserts was performed using a shuttle strategy modified from the method of Koh et al. (24). Five micrograms of genomic DNA was digested using 50 units of either NotI (Roche) or AscI (New England Biolabs) O/N in 100 μl, followed by an additional 3-h digestion upon the addition of 25 units. For each analyzed colony, both digestions were performed. Subsequently, fragments were purified using phenol-chloroform-isoamyl alcohol extraction and ethanol precipitated in the presence of 200 μg of type VII mussel glycogen (catalog no. G1508; Sigma) at −80°C. Ligation was performed O/N at 16°C in a total volume of 200 μl using 2 units of T4 DNA ligase (Roche) and in the presence of extra ATP to a concentration of 0.05 mM. An extra 3-h ligation was performed the next day upon the addition of 2 units of T4 DNA ligase. Ligated plasmids were purified as described above, electroporated in 5 μl of DH10B electromax competent cells per reaction (Invitrogen/Life Technologies), and plated on LB plates containing 5 μg of NaCl/liter and 100 μg of zeocin/ml (Invitrogen/Life Technologies). Colonies were propagated, and plasmids were isolated according to standard protocols. Sequencing was performed using the following primers: FW (5′ CAC CCC CAC CGC CCT CAA AGT AG 3′) and RV (5′ GGA ACG GCA CTG GTC AAC TTG G 3′).

MEF injections in immunocompromised mice. A total of 1×10^6 MEFs were suspended in 200 μl PBS and injected into immunocompromised BALB/c nude mice. Mice were inspected twice a week.

Protein isolation, immunoblot, immunoprecipitation, and in vitro kinase assays. For protein isolations, cells were lysed for 30 min on ice in lysis buffer containing 150 mM NaCl, 50 mM HEPES (pH 7.5), 5 mM EDTA, 0.1% NP-40, 5 mM NaF, 0.5 mM vanadate, 20 mM β-glycerolphosphate, and 1 tablet complete protease inhibitor cocktail (Roche) per 50 ml. After centrifugation, protein concentration was determined using Bio-Rad protein assay. For immunoblot analysis, 20 to 30 μg protein was separated on 12% SDS-polyacrylamide gels. Blotting was performed by using standard protocols. For immunoprecipitation reactions, lysates were incubated with antibody and 50% beads in lysis buffer (either protein A [Pharmacia] or protein A/G [Santa Cruz Biotechnology], depending on the antibody used) and incubated O/N at 4°C while rotating. Prior to immunoblot analysis, lysates were washed five times in lysis buffer and loaded on 12% SDS-polyacrylamide gels. Prior to kinase assays, lysates were washed three times in lysis buffer and then washed two times in kinase buffer containing 50 mM HEPES (pH 7.5), 5 mM $MgCl_2$, 2.5 mM $MnCl_2$, and 1 mM dithiothreitol. Kinase assays were performed by incubating 50 μg protein (CDK2 assay) or 20 μg protein (cyclin B1 kinase assay) with 5 μg histone H1 (Roche) and 2.5 μCi [γ-^{32}P]ATP in kinase buffer for 30 min at 37°C while shaking. After the reaction was stopped by adding protein loading buffer, one-third of this mixture was separated on 10% SDS-polyacrylamide gels, blotted by using standard protocols, and exposed to Kodak BioMax XAR films. The antibodies used for immunoblot analysis were mouse monoclonal anti-p21^{CIP} (F-5, SC-6246; Santa Cruz), mouse monoclonal anti-Ras (catalog no. 610002; BD Transduction Laboratories), sheep polyclonal anti-p53 (Ab-7, PC35; Calbiochem), rabbit anti-TBX2 (kindly provided by M. van Lohuizen), rabbit polyclonal anti-p19^{ARF} (ab80; Abcam), and goat polyclonal anti-CDK4 (C-22, SC-260-G; Santa Cruz Biotechnology). Secondary antibodies were horseradish peroxidase-conjugated goat anti-mouse, goat anti-rabbit, and rabbit anti-goat antibodies (DakoCytomation). The antibodies used for immunoprecipitation reactions were rabbit anti-CDK2 (M2; Santa Cruz), mouse anti-cyclin B1 (GNS1; Santa Cruz) for kinase assays, and rabbit anti-cyclin B1 (H433; Santa Cruz) for immunoblots. Immunoprecipitation reactions for cyclin B1 kinase assay were performed using protein A/G beads (Santa Cruz). All other immunoprecipitation reactions were performed using protein A beads (Pharmacia).

FACS analysis. For fluorescence-activated cell sorting (FACS) analysis, cells were trypsinized and fixed in 70% ethanol in PBS at 4°C. Subsequently, cells were washed in PBS, suspended in PBS containing 200 μg/ml RNase A and 20 μg/ml propidium iodide, incubated at 37°C for 15 min, and analyzed using Cell Quest and Summit software.

RESULTS

Gain-of-function screen for anchorage-independent growth of Ras^{V12}-expressing pocket protein-deficient MEFs. We have previously shown that ablation of pRb and p107 rendered MEFs insensitive to replicative and Ras^{V12}-induced senescence but was not sufficient for Ras^{V12}-induced transformation: Ras^{V12}-expressing DKO MEFs were unable to exhibit anchorage-independent growth in culture and did not form tumors in nude mice (7, 32). To identify events enabling Ras^{V12}-induced transformation of pocket protein-deficient MEFs, we performed a gain-of-function screen using *Rb*$^{-/-}$ *p130*$^{-/-}$ (DKO) MEFs expressing Ras^{V12}. In short, DKO MEFs were retrovirally transduced with pBABE-Ras^{V12} and subsequently with the pEYK-MCF7 cDNA library or with pEYK-GFP. Transduced cells were then seeded in soft agar. Although some colonies appeared in the control vector-infected cells, infection with the pEYK-MCF7 library increased the number of colonies three times. Colonies were picked, and

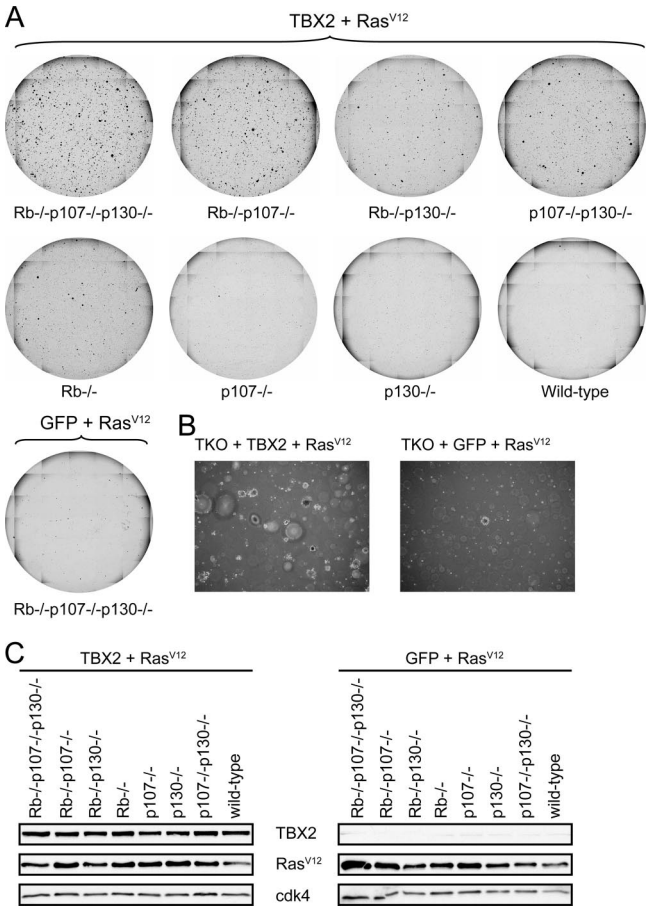

FIG. 1. TBX2 specifically transforms Ras^{V12}/pocket protein-deficient MEFs. (A) Primary MEFs of the indicated genotypes were first transduced with pEYK-TBX2 and subsequently with pBABE-Ras^{V12} (TBX2 + Ras^{V12}) and plated in soft agar. The left bottom dish shows $Rb^{-/-}$ $p107^{-/-}$ $p130^{-/-}$ MEFs infected with pEYK-GFP and pBABE-Ras^{V12} (GFP + Ras^{V12}). Pictures of soft agar plates were taken using a non-phase-contrast lens (×2.5 magnification). (B) Detailed pictures of $Rb^{-/-}$ $p107^{-/-}$ $p130^{-/-}$ (TKO) MEFs transduced with either pEYK-TBX2 or pEYK-GFP and subsequently with pBABE-Ras^{V12}. Pictures show the same cells as in panel A, taken using a phase-contrast lens (×5 magnification). (C) Ras^{V12} and TBX2 protein levels in the cell lines depicted in panels A and B. (Left) MEFs infected with pEYK-TBX2 and pBABE-Ras^{V12}. (Right) MEFs infected with pEYK-GFP and pBABE-Ras^{V12}.

the presence of a pEYK-cDNA integration was determined by both PCR analysis and by a shuttling method that enabled excision of the integrated pEYK-cDNA from the genomic DNA and its propagation as a plasmid in *Escherichia coli* (24). Sequencing of recovered pEYK vectors revealed many fragmented cDNA sequences in the sense or antisense orientation. Three independent colonies contained a full cDNA encoding the *TBX2* oncogene. Only reintroduction of the TBX2-expressing vector into pocket protein-deficient MEFs expressing Ras^{V12} caused robust colony formation in soft agar (Fig. 1A, compare left top and left bottom dishes).

TBX2 transforms pocket protein-deficient MEFs expressing Ras^{V12}. To determine whether transformation by TBX2 required the loss of specific pocket proteins, we retrovirally transduced MEFs deficient for all different combinations of pocket proteins with either pEYK-TBX2 or pEYK-GFP, followed by pBABE-Ras^{V12}, and tested their ability to form colonies in soft agar. In all the cell lines tested, expression of Ras^{V12} alone hardly induced anchorage-independent growth (see Fig. 1A and B for TKO MEFs; also data not shown). Concomitant expression of TBX2 induced colony formation in TKO, DKO, and $Rb^{-/-}$ MEFs (Fig. 1A and B). The strongest colony formation was observed with TKO MEFs, followed by $Rb^{-/-}$ $p107^{-/-}$ MEFs and then by $Rb^{-/-}$ $p130^{-/-}$, $p107^{-/-}$ $p130^{-/-}$, and $Rb^{-/-}$ MEFs. In contrast, expression of TBX2 and Ras^{V12} did not support anchorage-independent growth of $p107^{-/-}$, $p130^{-/-}$, and wild-type MEFs, the latter being consistent with previous results (21). Note that Ras^{V12} and TBX2 were expressed to comparable levels in all cell lines (Fig. 1C). Expression of TBX2 alone in pocket protein-deficient MEFs did not induce colony formation (data not shown). Together, these results indicate that the combination of pocket protein ablation, Ras^{V12} expression, and TBX2 expression is required for transformation of primary MEFs.

Transformation of TBX2/Ras^{V12}-expressing MEFs requires ablation of pocket proteins. To provide independent proof for collaboration between TBX2 and the loss of pocket proteins, we made use of $Rb^{F/F}$ $p130^{-/-}$ MEFs. In these cells, exon 19 of both *Rb* alleles is flanked by LoxP sites and can therefore be deleted by Cre-mediated recombination, which inactivates the gene. $Rb^{F/F}$ $p130^{-/-}$ MEFs were transduced with retroviral vectors expressing TBX2 and Ras^{V12} and subsequently with either pMSCV-Cre-ERT2 or empty pMSCV. Even without the addition of tamoxifen, transduction of Cre-ERT2 in $Rb^{F/F}$ $p130^{-/-}$ MEFs already resulted in nuclear Cre activity, yielding a mixed population of cells containing active (Rb^{F}) and/or inactive ($Rb^{\Delta 19}$) *Rb* alleles (Fig. 2A). Expression of Cre-ERT2 in TBX2/Ras^{V12}/$Rb^{F/F}$ $p130^{-/-}$ MEFs increased colony formation in soft agar, indicating that inactivation of the *Rb* allele promoted anchorage-independent growth (Fig. 2B). Conversely, expression of TBX2, Ras^{V12}, and Cre-ERT2 in $Rb^{+/+}$ $p130^{-/-}$ MEFs did not enhance colony formation (data not shown). Note that some colonies appeared in the control vector-infected cells (Fig. 2B, right part), which was probably due to the prolonged culturing required for transduction with three retroviral vectors, creating a window for the selection for additional growth-stimulating mutations. Soft agar colonies derived from $Rb^{F/F}$ $p130^{-/-}$ MEFs transduced with TBX2, Ras^{V12}, and Cre-ERT2 were picked and analyzed for *Rb* status by PCR. Strikingly, while the starting population of cells consisted of a mixed population carrying active and inactive *Rb* alleles (Fig. 2A), all 14 soft agar colonies exclusively carried inactive *Rb* alleles (Fig. 2C; note that 5 colonies failed to produce PCR fragments, probably due to the loss of cells during picking). Together with the results presented in Fig. 1, these experimental results show that transformation of MEFs by Ras^{V12} requires both ablation of pocket proteins and expression of TBX2.

Requirements for growth of MEFs in nude mice. To study transformation in an in vivo system, $Rb^{-/-}$ $p107^{-/-}$, $Rb^{-/-}$ $p130^{-/-}$, and $Rb^{-/-}$ $p107^{-/-}$ $p130^{-/-}$ MEFs were retrovirally transduced with either Ras^{V12} and TBX2 or Ras^{V12} and green fluorescent protein (GFP) and injected into immunocompromised mice (nude mice) (Fig. 3). TBX2 and Ras^{V12} expression levels were comparable in the different cell lines (data not

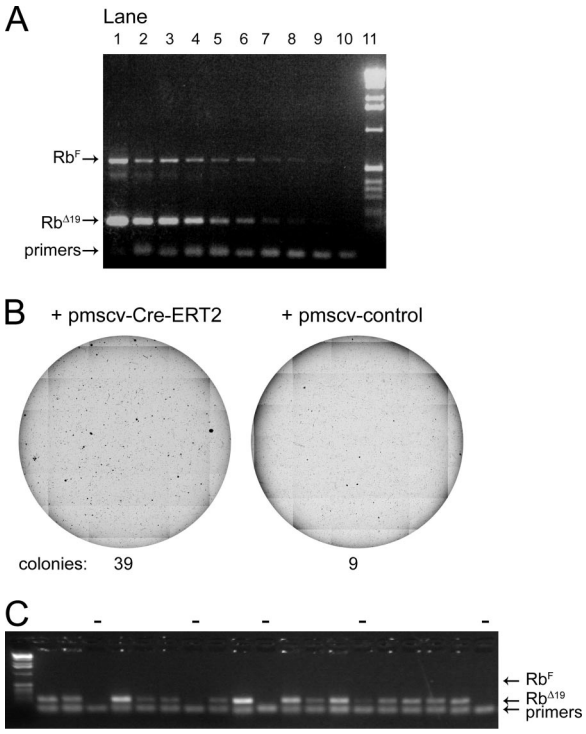

FIG. 2. Transformation by TBX2 and Ras^{V12} requires ablation of pocket proteins. (A) Expression of Cre-ERT2 yields a mixed population of cells containing active (Rb^F) and/or inactive ($Rb^{\Delta 19}$) *Rb* alleles. $Rb^{F/F}$ $p130^{-/-}$ MEFs were transduced with TBX2, Ras^{V12}, and pMSCV-Cre-ERT2 viruses. Genomic DNA (gDNA) was isolated and analyzed for the presence of active and inactive Rb by PCR. Lane 1, 100 ng of input gDNA; lanes 2 to 10, genomic DNA diluted 2-, 4-, 8-, 16-, 32-, 64-, 128-, 256-, and 512-fold, respectively, showing that both alleles could be detected at a low input concentration of gDNA; lane 11, 1-kilobase ladder. (B) Expression of Cre-ERT2 enhances colony formation in $Rb^{F/F}$ $p130^{-/-}$ MEFs. $Rb^{F/F}$ $p130^{-/-}$ MEFs infected with TBX2 and Ras^{V12} and either pMSCV-Cre-ERT2 (left) or pMSCV-empty (right) viruses were plated in soft agar. Pictures were taken using a non-phase-contrast lens (×2.5 magnification). (C) Nineteen soft agar colonies derived from $Rb^{F/F}$ $p130^{-/-}$ MEFs expressing TBX2, Ras^{V12}, and Cre-ERT2 were picked and immediately analyzed for the presence of active and inactive *Rb* by PCR. Each lane represents one soft agar colony; the leftmost lane contains a 1-kilobase ladder. Five colonies (−) failed to produce PCR fragments. The positions of active and inactive *Rb* alleles are indicated by Rb^F and $Rb^{\Delta 19}$.

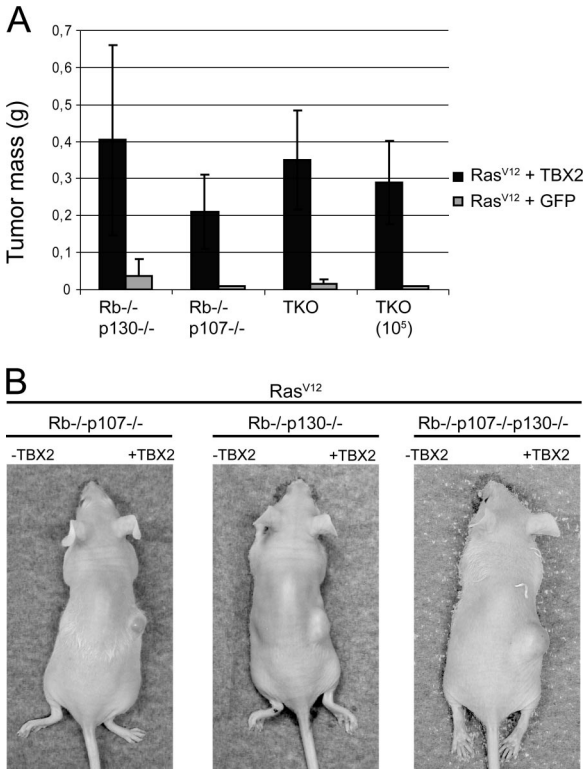

FIG. 3. Expression of TBX2 promotes tumor formation of pocket protein-deficient MEFs expressing Ras^{V12}. Immunocompromised mice (nude mice) were injected with MEFs of the indicated genotypes, which had been transduced with either pBABE-Ras^{V12} and pEYK-GFP (Ras^{V12} + GFP) (injected into the left flanks) or pBABE-Ras^{V12} and pEYK-TBX2 (Ras^{V12} + TBX2) (injected into the right flanks). Unless indicated, 10^6 MEFs were injected per flank. Three mice were injected per cell line; two additional mice were injected with 10^5 $Rb^{-/-}$ $p107^{-/-}$ $p130^{-/-}$ (TKO) MEFs. (A) Graphical representation of tumor mass. Error bars denote standard deviations. (B) Pictures of immunocompromised mice injected with MEFs of the indicated genotypes. MEFS were transduced with either pEYK-TBX2 (+TBX2) or with pEYK-GFP (−TBX2).

shown). $Rb^{-/-}$ $p107^{-/-}$ $p130^{-/-}$ MEFs expressing Ras^{V12} and TBX2 formed tumors within a shorter time window than $Rb^{-/-}$ $p107^{-/-}$ or $Rb^{-/-}$ $p130^{-/-}$ MEFs expressing Ras^{V12} and TBX2; mice injected with TKO MEFs had to be sacrificed between 16 and 21 days, while mice injected with DKO MEFs were sacrificed after 26 days. This suggests, consistent with the soft agar experiments (Fig. 1), that MEFs deficient for all three pocket proteins were more easily transformed than MEFs partially deficient for pocket proteins. DKO and TKO MEFs expressing Ras^{V12} and TBX2 formed robust tumors, weighing between 0.1 and 0.7 g upon dissection. In contrast, MEFs expressing Ras^{V12} and GFP formed very small clumps of cells, in 9 out of 11 cases weighing less than 0.01 g. In the other two cases, small tumors were formed; these tumors were 10 and 4 times smaller than the corresponding tumors expressing Ras^{V12}/TBX2. These results demonstrate that also in vivo, expression of TBX2 strongly supports transformation of Ras^{V12}-expressing DKO and TKO MEFs.

Downregulating the p53 pathway transforms pocket protein-deficient MEFs. Overexpression of TBX2 induces bypass of both replicative and Ras^{V12}-induced senescence. This has been attributed to downregulation of $p19^{ARF}$, and as a consequence, to downregulation of p53 (9, 21). Furthermore, TBX2 has been reported to directly repress the promoter of the *p53* target gene $p21^{CIP1}$ (33, 44). Given the importance of p53 in transformation, we investigated whether TBX2-induced transformation could be attributed to downregulation of the p53/$p21^{CIP1}$ pathway. To this aim, we expressed a pBABE-$p21^{CIP1}$ vector in TKO MEFs expressing TBX2 and Ras^{V12}. Ectopic expression of $p21^{CIP1}$ dramatically reduced the number of soft agar colonies induced by TBX2 (see Fig. S1 in the supplemental material), indicating that TBX2-induced transformation involves downregulation of $p21^{CIP1}$.

To further address the involvement of downregulating the p53/$p21^{CIP1}$ pathway in transformation, we used pRetroSuper (pRS) vectors to suppress expression of p53 or $p21^{CIP1}$ in DKO

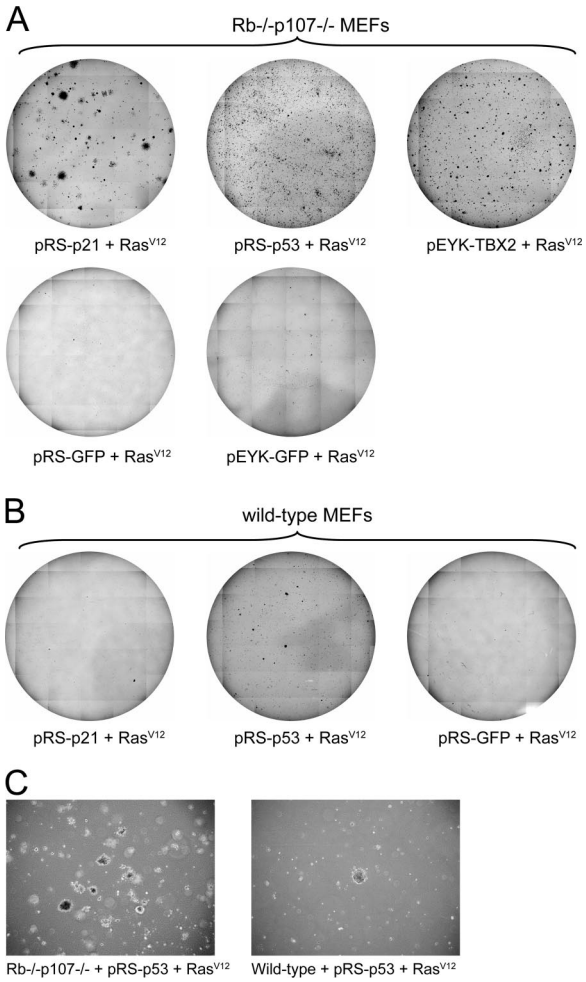

FIG. 4. Similar to TBX2 overexpression, downregulation of either p21^{CIP1} or p53 specifically transforms pocket protein-deficient MEFs. (A) *Rb*$^{-/-}$ *p107*$^{-/-}$ MEFs were transduced with the indicated constructs and plated in soft agar. Pictures were taken using a non-phase-contrast lens (×2.5 magnification). (B) Wild-type MEFs were transduced with the indicated constructs and plated in soft agar. Pictures were taken using a non-phase-contrast lens (×2.5 magnification). (C) Detailed pictures of the indicated cell lines, plated in soft agar. Pictures show the same cells as in panels A and B, taken using a phase-contrast lens (×5 magnification).

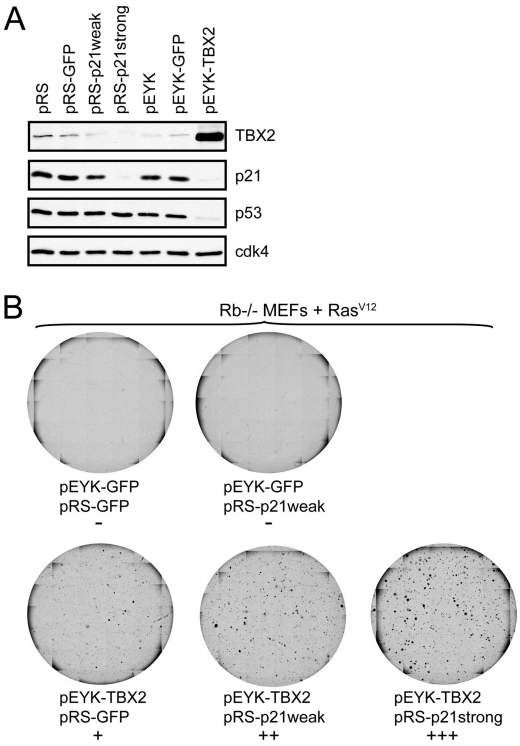

FIG. 5. A balance between the activities of the pocket protein and p21^{CIP1} pathways determines the level of transformation of MEFs. (A) Downregulation of p21^{CIP1} using various constructs. *Rb*$^{-/-}$ *p107*$^{-/-}$ MEFs were infected with the indicated constructs and plated in suspension culture 6 days postinfection. After 24 h, cells were harvested, lysed, and immunoblotted for the indicated proteins. (B) *Rb*$^{-/-}$ MEFs were first infected with pEYK-GFP or pEYK-TBX2, next with pRS-GFP or a pRS-p21 vector, and last with pBABE-Ras^{V12}. Forty-eight hours postinfection, cells were plated in soft agar. Pictures were taken using a non-phase-contrast lens (×2.5 magnification). + and − symbols refer to the quantification of colony formation as depicted in Table 1.

MEFs by RNA interference. Similar to overexpression of TBX2, downregulation of either p53 or p21^{CIP1} supported anchorage-independent growth of Ras^{V12}-expressing *Rb*$^{-/-}$ *p107*$^{-/-}$ MEFs (Fig. 4A). Knockdown of p53 was more potent in inducing anchorage-independent growth than knockdown of p21^{CIP1} was. Residual levels of p21^{CIP1} were comparable or even somewhat higher in p53 knockdown cells (see Fig. 6D), suggesting that p53 protects against anchorage-independent growth only partially via p21^{CIP1}. As observed for transformation by TBX2, transformation by p21^{CIP1} knockdown required pocket protein loss; p21^{CIP1} downregulation and Ras^{V12} expression in wild-type MEFs did not induce colony formation in soft agar (Fig. 4B). Although p53 downregulation and Ras^{V12} expression in wild-type MEFs induced a small number of colonies (Fig. 4B), this sharply contrasted to the robust colony formation observed for Ras^{V12}/*Rb*$^{-/-}$ *p107*$^{-/-}$ MEFs (Fig. 4C). These results show that in a Ras^{V12} transformation assay, downregulation of the p53 pathway mimics overexpression of TBX2. Similar as observed for TBX2, transformation by downregulation of the p53 pathway requires the loss of pocket proteins.

A balance between the p53 pathway and the pocket protein pathway determines the level of transformation of MEFs. Since colony formation in TBX2/Ras^{V12}-expressing MEFs was more robust upon the loss of two or three pocket proteins compared to the loss of pRB alone (Fig. 1) and transformation by TBX2 could be attributed to downregulation of the p53/p21^{CIP1} pathway (Fig. 4), we hypothesized that a balance between the activities of the pocket protein and the p53/p21^{CIP1} pathways determines the rate of transformation of MEFs. We therefore used pRS vectors downregulating p21^{CIP1} to different levels, referred to as pRS-p21weak and pRS-p21strong. Figure 5A shows that infection with pRS-p21weak in *Rb*$^{-/-}$ *p107*$^{-/-}$ MEFs caused a mild decrease of p21^{CIP1} levels compared to infection with control vectors (pRS or pRS-GFP), while infection with pRS-p21strong caused a strong decrease. We downregulated p21^{CIP1} to different degrees by combined expression of the pRS-p21 vectors and the pEYK-TBX2 ex-

TABLE 1. Summary of growth of the cell lines in soft agar[a]

Genotype of cell line	Growth[b] in soft agar of cell line infected with the following construct:				
	Control vector	pRS-p21weak	pEYK-TBX2	pEYK-TBX2 + pRS-p21weak	pEYK-TBX2 + pRS-p21strong
Wild-type	−	−	−	−	+/−
$Rb^{-/-}$	−	−	+	++	+++
$Rb^{-/-}$ $p107^{-/-}$	−	−	++++	++++	++++
TKO	+/−	+/−	+++++	+++++	+++++

[a] A balance between the activities of the pocket protein and $p21^{CIP1}$ pathways determines the level of transformation of MEFs. Cells were infected as described in the legend to Fig. 5, plated in soft agar, and monitored for anchorage-independent growth.

[b] Symbols: −, no growth; +/−, less than 20 colonies; +, ++, +++, ++++, and +++++, indicate the relative capacity for growth in soft agar, where each additional + indicates an approximately twofold increase. +, ++, and +++ correspond to the levels of soft agar growth shown in Fig. 5B.

pression vector in MEFs deficient for different combinations of pocket proteins. Briefly, TKO MEFs, $Rb^{-/-}$ $p107^{-/-}$ MEFs, $Rb^{-/-}$ MEFs, and wild-type MEFs were first infected with pEYK-GFP or pEYK-TBX2, subsequently with pRS-GFP or a pRS-p21 vector, and finally with pBABE-Ras^{V12}. The colony-forming capacity in soft agar was monitored, and the results are summarized in Table 1. Expression of Ras^{V12} and TBX2, without additional $p21^{CIP1}$ downregulation, induced colony formation most robustly in TKO MEFs, followed by $Rb^{-/-}$ $p107^{-/-}$ and $Rb^{-/-}$ MEFs, but expression of Ras^{V12} and TBX2 did not induce colony formation in wild-type MEFs (Table 1 and Fig. 1). Strikingly, in $Rb^{-/-}$ MEFs, coexpression of the pRS-p21 vectors enhanced TBX2-induced colony formation (Fig. 5B). These results show that relatively mild $p21^{CIP1}$ downregulation was sufficient to induce transformation of MEFs with complete pocket protein loss (pEYK-TBX2 expression in Ras^{V12}/TKO MEFs), while strong $p21^{CIP1}$ downregulation was required to induce transformation of MEFs partially deficient for pocket proteins (pEYK-TBX2 plus pRS-p21strong in Ras^{V12}/$Rb^{-/-}$ MEFs). Thus, a balance between pocket protein and $p21^{CIP1}$ levels determines the rate of transformation of Ras^{V12}-expressing MEFs.

Ras^{V12}-induced transformation of pocket protein-deficient MEFs requires rescue of G_2 arrest. Whereas under adherent conditions, the loss of pocket proteins turned Ras^{V12} expression from a growth-inhibiting signal to a growth-promoting signal, Ras^{V12}/TKO MEFs were largely unable to form colonies in soft agar. To determine why proliferation ceased upon removal of anchorage, we analyzed the cell cycle profile of anchorage-deprived DKO and TKO MEFs by FACS. For this experiment, we cultured cells in methylcellulose, which like soft agar, prohibits attachment but enables easy recovery of nonproliferating cells. Upon removal of anchorage, wild-type fibroblasts arrest in G_1 (10, 14, 15). Here, we show that the majority of Ras^{V12}/$Rb^{-/-}$ $p107^{-/-}$ MEFs arrested in both G_1 and G_2 upon removal of anchorage (Fig. 6A). Knockdown of $p21^{CIP1}$ reduced the fraction of G_2 cells (Fig. 6A). As the number of S-phase cells remained low, this indicates that a large fraction of the cells had arrested in G_1. In contrast, knockdown of p53 increased the number of S-phase cells, indicating rescue of both G_1 and G_2 arrest in nonadherent cells (Fig. 6A). Ras^{V12}/TKO MEFs predominantly arrested in G_2 upon removal of anchorage, which could be alleviated by knockdown of $p21^{CIP1}$ or p53 (Fig. 6B) or by overexpression of TBX2 (Fig. 6C). Note that G_2 arrest under nonadherent conditions in Ras^{V12}/TKO MEFs was not induced by expression of Ras^{V12}, as TKO MEFs also arrested in G_2 upon removal of anchorage (see Fig. S2 in the supplemental material). Similar to knockdown of p53 or $p21^{CIP1}$, knockdown of $p19^{ARF}$ also rescued G_2 arrest in nonadherent Ras^{V12}/TKO MEFs (Fig. 7C; note that while the vector used targets the *INK4A/ARF* locus, the effect was due to knockdown of $p19^{ARF}$, as downregulation of $p16^{INK4A}$ alone did not rescue G_2 arrest of Ras^{V12}/TKO MEFs). As TBX2 expression downregulated $p19^{ARF}$ (Fig. 7A), these results suggest that transformation by TBX2 involved downregulation of $p19^{ARF}$, and subsequently p53 and $p21^{CIP1}$. In conclusion, our results demonstrate that the loss of anchorage induces checkpoint activation in G_1 and G_2, the latter becoming more prominent upon the loss of pocket proteins. Transformation requires rescue of cell cycle arrest, which can be achieved by expression of TBX2 or downregulation of the $p19^{ARF}$/p53/$p21^{CIP1}$ pathway.

Downregulating the p53/$p21^{CIP1}$ pathway by TBX2 expression or RNA interference rescues cyclin-dependent kinase activities under nonadherent conditions. As the G_1/S and G_2/M transitions require cyclin E-CDK2 and cyclin B1-CDK1, respectively, we analyzed the activity of these complexes under nonadherent conditions. Figure 8A shows that expression of TBX2 induced cyclin B1- and CDK2-associated kinase activities in Ras^{V12}-expressing TKO cells under nonadherent conditions (Fig. 8, panels 1 and 2). Increased kinase activity in TBX2-expressing cells was related to reduced association of $p21^{CIP1}$ with cyclin B1 and CDK2 (Fig. 8, panels 3 and 4). This is most likely due to reduction of p53 levels by TBX2 (Fig. 8, panels 5, 6, and 7). These results indicate that expression of TBX2 relieves inhibition of cyclin-dependent kinase activity by $p21^{CIP1}$, leading to rescue of cell cycle arrest and anchorage-independent growth.

Downregulating the p53/$p21^{CIP1}$ pathway transformed DKO and TKO MEFs more effectively than $Rb^{-/-}$ MEFs (Fig. 1 and Table 1). We therefore compared the regulation of cyclin-dependent kinase activities in $Rb^{-/-}$ and $Rb^{-/-}$ $p107^{-/-}$ MEFs under both adherent and nonadherent conditions. Both cell lines were infected with either pRS-p21 or pRS-GFP and then with pBABE-Ras^{V12} and plated either in methylcellulose or under adherent conditions. Cyclin B1- and CDK2-associated kinase activities in $Rb^{-/-}$ $p107^{-/-}$ MEFs were higher than in $Rb^{-/-}$ MEFs, which was particularly visible under adherent conditions (Fig. 8B, compare lanes 1 and 3 and lanes 5 and 7). The loss of anchorage caused inhibition of kinase activities in $Rb^{-/-}$ and $Rb^{-/-}$ $p107^{-/-}$ MEFs (Fig. 8B, compare lanes 1 and 5 and lanes 3 and 7). Knockdown of $p21^{CIP1}$ induced

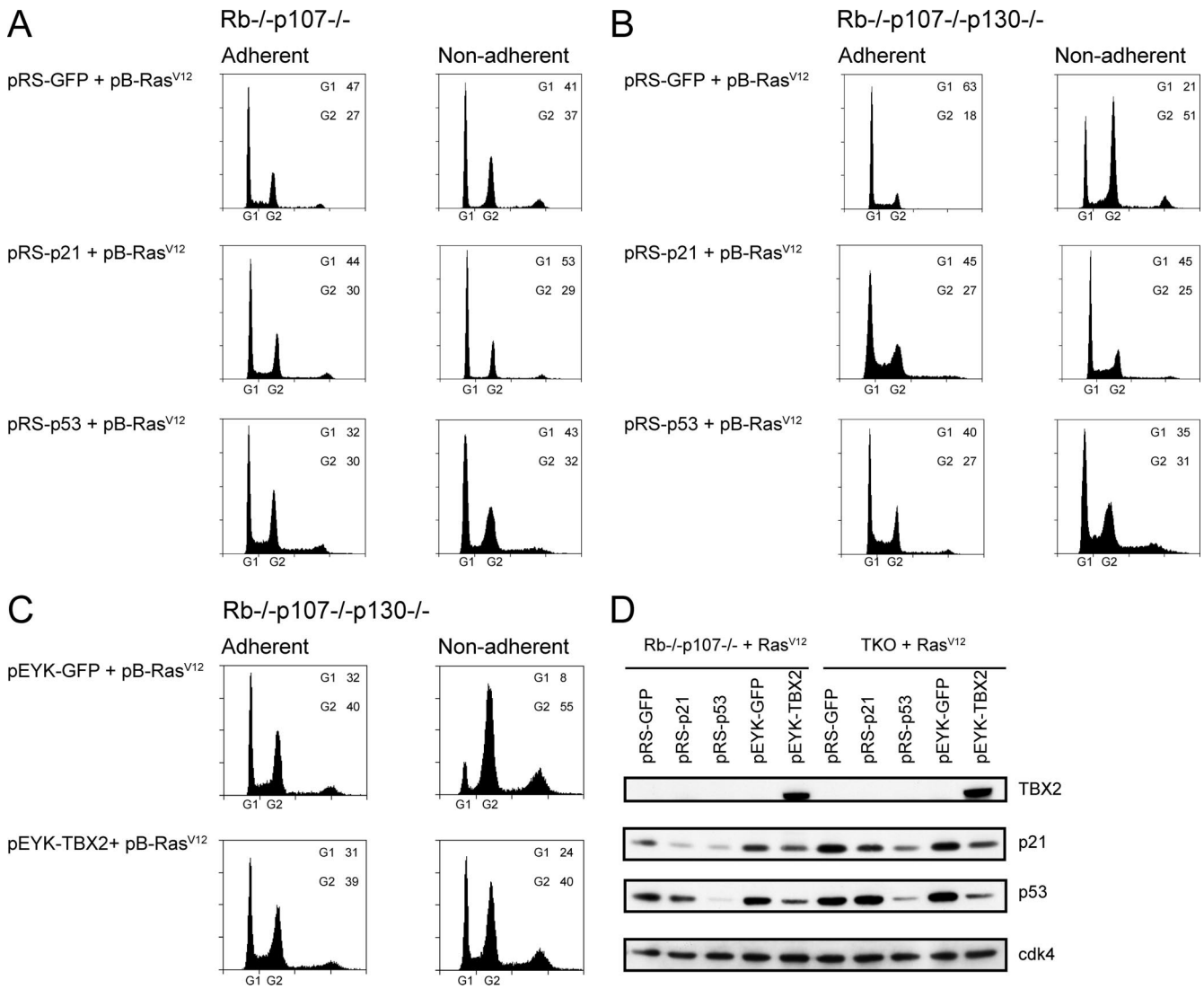

FIG. 6. Anchorage-independent growth of Ras^{V12}/pocket protein-deficient MEFs requires rescue of G_2 arrest. $Rb^{-/-}$ $p107^{-/-}$ MEFs (A) or $Rb^{-/-}$ $p107^{-/-}$ $p130^{-/-}$ (TKO) MEFs (B and C) were infected with the indicated constructs and cultured either under adherent conditions or for 6 days in methylcellulose. Cells were harvested, stained with propidium iodide, and analyzed by FACS. The percentages of cells in G_1 and G_2 are shown in the top right corners of graphs. (D) Downregulation of $p21^{CIP1}$ and p53 in $Ras^{V12}/Rb^{-/-}$ $p107^{-/-}$ and Ras^{V12}/TKO MEFs upon infection with the indicated constructs. Cells were plated in suspension culture for 24 h, lysed, and immunoblotted for the indicated proteins.

kinase activities under both adherent and nonadherent conditions, and as expected, no association of $p21^{CIP1}$ with CDK2 could be detected (Fig. 8B, lanes 2, 4, 6, and 8). However, in nonadherent $Ras^{V12}/Rb^{-/-}$ MEFs (Fig. 8B, lane 6), the increase in CDK2 and cyclin B1-associated kinase activity was minor and apparently not sufficient to support anchorage-independent growth. In contrast, knockdown of $p21^{CIP1}$ in $Ras^{V12}/Rb^{-/-}$ $p107^{-/-}$ MEFs (Fig. 8B, lane 8) raised kinase activities to much higher levels than observed in $Ras^{V12}/Rb^{-/-}$ MEFs (lane 6). Note that knockdown of $p21^{CIP1}$ induced cyclin B1-associated kinase activity more robustly than CDK2-associated kinase activity. This fits with the observation that knockdown of $p21^{CIP1}$ was more potent in rescuing G_2 arrest than in rescuing G_1 arrest (Fig. 6). We conclude that downregulation of $p21^{CIP1}$ sufficiently rescued the decrease in kinase activities induced by the loss of adhesion only in $Ras^{V12}/Rb^{-/-}$ $p107^{-/-}$ MEFs. This allowed bypass of G_2 arrest and, to a lower extent, G_1 arrest, enabling anchorage-independent growth.

DISCUSSION

Pocket protein depletion is not sufficient for Ras^{V12}-induced transformation of MEFs. Functional inactivation of the pocket protein and p53 tumor suppressor pathways is one of the most frequent events in the development of cancer. Consistent with their importance in G_1 control, the loss of either p53 or pocket proteins bypasses replicative senescence in primary murine embryonic fibroblasts (7, 8, 19, 38). Furthermore, inactivation of the p53 pathway or the loss of pRb and at least one other pocket protein reversed the growth-inhibitory effect of Ras^{V12} into a proliferative stimulus (32, 39). However, unlike abrogation of p53, the loss of pocket proteins was not sufficient to

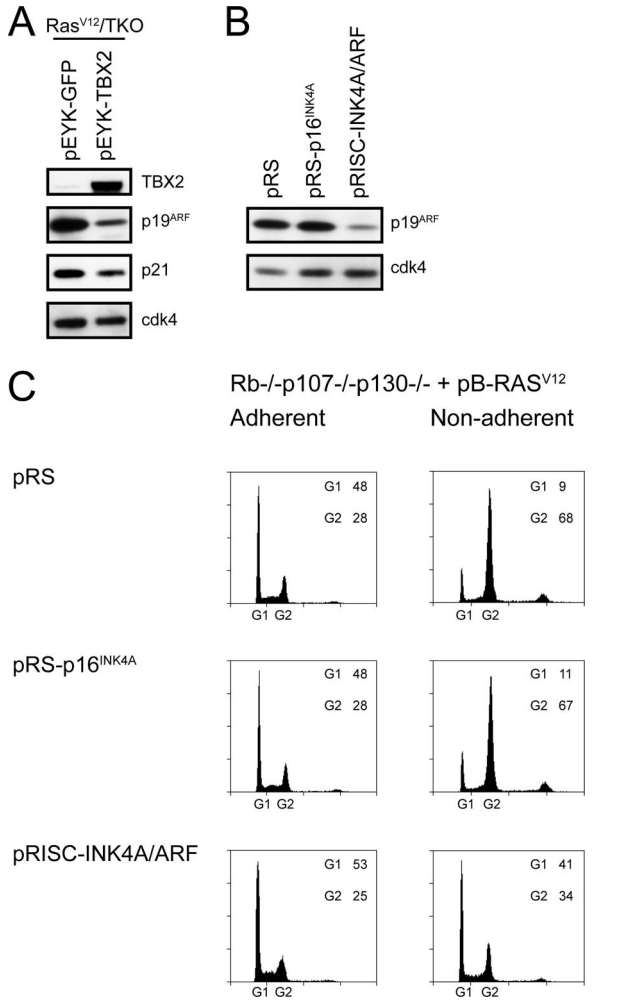

FIG. 7. Transformation by TBX2 involves downregulation of p19^{ARF}. (A) TBX2 downregulates p19^{ARF} in RAS^{V12}/TKO MEFs. (B) Downregulation of p19^{ARF} by a knockdown vector targeting the *INK4A/ARF* locus, but not by a vector targeting p16^{INK4A}. (C) p19^{ARF} downregulation rescues G_2 arrest in nonadherent Ras^{V12}/TKO MEFs. Cells were infected with the indicated constructs and cultured under adherent conditions or for 5 days in methylcellulose. Cells were harvested, stained with propidium iodide, and analyzed by FACS. The percentages of cells in G_1 and G_2 are shown in the top right corners of graphs.

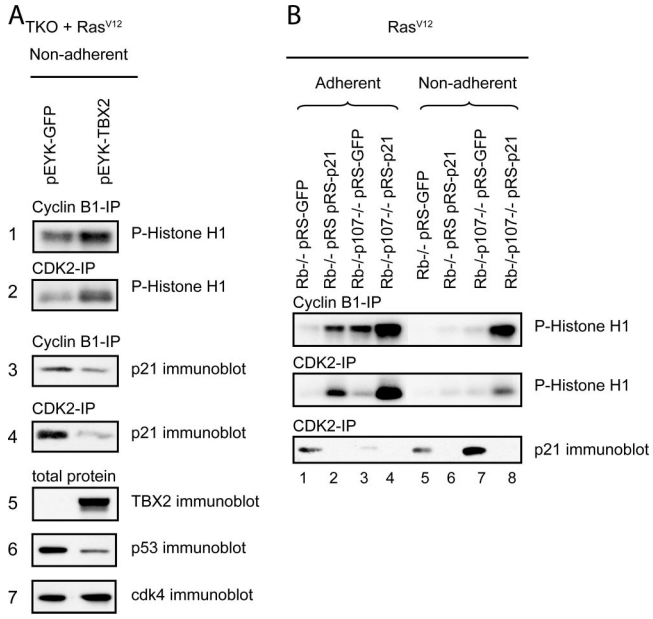

FIG. 8. A combination of pocket protein loss and downregulation of the p53/p21^{CIP1} pathway rescues cyclin-dependent kinase activities under nonadherent conditions. (A) *Rb*$^{-/-}$ *p107*$^{-/-}$ *p130*$^{-/-}$ (TKO) MEFs infected with pBABE-Ras^{V12} (Ras^{V12}) and either pEYK-TBX2 or pEYK-GFP were cultured in methylcellulose for 6 days. (Panels 1 and 2) Cyclin B1- and CDK2-associated kinase activities as determined by in vitro phosphorylation of histone H1. IP, immunoprecipitate; P-Histone H1, phosphorylated histone H1. (Panels 3 and 4) Cyclin B1 and CDK2 immunoprecipitates were immunoblotted for p21^{CIP1}. (Panels 5, 6, and 7) Total protein levels of TBX2, p53, and CDK4 as loading control. (B) *Rb*$^{-/-}$ and *Rb*$^{-/-}$ *p107*$^{-/-}$ MEFs infected with either pRS-p21 or pRS-GFP and subsequently with pBABE-Ras^{V12} were cultured under adherent conditions or in methylcellulose for 5 days. Cyclin B1- and CDK2-associated kinase activities as well as association of p21^{CIP1} with CDK2 are shown in the top, middle, and bottom panels, respectively.

support oncogenic transformation by Ras^{V12} (32). This observation contradicts a report by others (38) but is strongly confirmed in the present study; Ras^{V12}-expressing MEFs deficient for both pRb and p130, both pRb and p107, or all three pocket proteins were largely unable to exhibit anchorage-independent growth or to form tumors in nude mice. By screening a cDNA library, we have identified a missing link: overexpression of the *TBX2* oncogene strongly induced transformation of pocket protein-deficient MEFs by Ras^{V12}, as evidenced by anchorage-independent growth in vitro and in vivo (Fig. 1 and 3). We have consistently shown that transformation of MEFs overexpressing TBX2 and Ras^{V12} required the loss of pocket proteins (Fig. 2). These results show that the loss of pocket proteins and overexpression of TBX2 strongly act synergistically in Ras^{V12}-induced transformation of primary murine embryonic fibroblasts.

The pRB and p53 pathways cooperate in suppression of transformation. TBX2 overexpression is known to attenuate the p53/p21^{CIP1} tumor suppressor pathway by downregulating transcription of the Mdm2 inhibitor p19^{ARF}. Consistently, we show that partial RNA interference-mediated knockdown of p19^{ARF}, p53, or p21^{CIP1} strongly supported Ras^{V12}-induced transformation of pocket protein-deficient MEFs (Fig. 4A, 6, and 7). Moreover, expression of p21^{CIP1} inhibited TBX2-induced transformation (see Fig. S1 in the supplemental material). The complete loss of p53 was sufficient for Ras^{V12}-induced transformation of wild-type MEFs (32). Here we show that partial knockdown of p53 induced anchorage-independent growth only to a very limited degree in wild-type MEFs but was very effective in pocket protein-deficient MEFs (Fig. 4B and C). Furthermore, we found that anchorage-independent growth upon Ras^{V12} expression could be achieved by either a combination of moderate p21^{CIP1} downregulation and severe pocket protein loss or strong p21^{CIP1} downregulation and mild pocket protein loss (Fig. 5 and Table 1). Apparently, the p53 and pRB pathways act synergistically in preventing anchorage-independent growth.

The complete loss of pocket proteins did not support anchorage-independent growth upon expression of Ras^{V12}, although it should be noted that a small number of colonies appeared in the soft agar culture. This may be explained by downregulation of the p53/$p21^{CIP1}$ pathway in a subset of the cells. Indeed, Sage and coworkers (38) reported that two out of five TKO MEF cultures displayed downregulation of p53 and $p21^{CIP1}$ during culturing under adherent conditions.

Regulation of cell cycle arrest and cyclin-dependent kinase activity by pRB, TBX2, and p53. Anchorage-independent growth is a hallmark of transformed cells. Untransformed cells are dependent on anchorage via integrin signaling. Upon attachment to the extracellular matrix, integrin signaling induces cyclin D1 and inhibits $p21^{CIP1}$ and $p27^{KIP1}$ expression, thereby authorizing cell cycle progression (1, 37, 47). Conversely, detachment from the extracellular matrix is associated with downregulation of cyclin D1, induction of $p21^{CIP1}$ and $p27^{KIP1}$, and increased association of $p21^{CIP1}$ and $p27^{KIP1}$ with cyclin-CDK complexes (10, 49, 50). As a result, cells deprived of attachment downregulate CDK2 activity and arrest in G_1 (10, 15). We show here that in anchorage-deprived Ras^{V12}/DKO MEFs, there was only partial G_1 arrest, as a substantial fraction of cells arrested in G_2 (Fig. 6A). In Ras^{V12}/TKO MEFs, which have completely lost the G_1 restriction point, G_2 arrest predominated (Fig. 6B). Thus, anchorage dependence is regulated via both G_1 and G_2 checkpoints. Our results therefore indicate that the transforming activity of TBX2 not only relies on override of the G_1 checkpoint but also on override of the G_2 checkpoint and involves downregulation of the p53 pathway (Fig. 6).

Are G_2-arrested cells senescent? We were unable to perform a senescence-associated β-galactosidase staining on arrested cells, as both DKO and TKO MEFs were targeted with a *lacZ* reporter gene. However, we have strong indications that the arrest is reversible, which according to the current definition excludes senescence. To address this issue, we centrifuged Ras^{V12}/TKO MEFs harvested from methylcellulose at low speed to separate the low number of growing colonies from G_2-arrested cells. By FACS, we found that the population of cells in the supernatant was enriched for G_2-phase cells. These cells entered the cell cycle upon reattachment, as observed by growth of the cells and by FACS profiles (data not shown).

The level of $p21^{CIP1}$ knockdown required to induce transformation was dependent on the extent of pocket protein ablation: relatively moderate $p21^{CIP1}$ knockdown was sufficient to induce anchorage-independent growth in TKO MEFs, whereas strong $p21^{CIP1}$ knockdown was required to transform *Rb*-deficient MEFs. Our results indicate that these different requirements for anchorage-independent growth are due to different levels of kinase activities in pocket protein-ablated cells. Despite high levels of cyclins A, E, and B1 in $Rb^{-/-}$ MEFs (6, 12, 20, 26), their associated kinase activities were lower than in $Rb^{-/-}$ $p107^{-/-}$ MEFs (Fig. 8), and this may be caused by E2F-dependent induction of p107 (48). As Rodier and coworkers (36) suggested that overexpression of p107 reduces the half-life of Skp2 protein, this could lead to downregulation of Skp2 in $Rb^{-/-}$ MEFs and subsequently, inhibition of $p27^{KIP1}$ degradation. However, we did not observe different $p27^{KIP1}$ levels in $Rb^{-/-}$ and $Rb^{-/-}$ $p107^{-/-}$ MEFs (data not shown). An alternative may be that high p107 levels in $Rb^{-/-}$ cells, together with p130, inhibit kinase activities in $Rb^{-/-}$ MEFs via direct binding to cyclin E-A/CDK2 (5, 13). This mechanism may explain why the extent of $p21^{CIP1}$ knockdown needed to achieve sufficient cyclin-dependent kinase activity to support anchorage-independent growth was lower in DKO and TKO MEFs than in $Rb^{-/-}$ cells. In conclusion, we propose that the pocket protein and p53 pathways synergistically protect against anchorage-independent growth by their shared ability to regulate cyclin-dependent kinase activities.

Roles of pRB, TBX2, and p53 in tumorigenesis. We identified *TBX2* as a transforming oncogene in pocket protein-deficient cells. Several lines of evidence point to a role for TBX2 during in vivo tumorigenesis. TBX2 was found amplified in a range of human tumor samples and cancer cell lines of different developmental origin, such as melanoma cell lines (44), a subset of human breast tumors (21, 43), and pancreatic cancer cell lines (27). The combined loss of components of the pRB and p53 pathways cooperates in tumorigenesis in vivo. The loss of $p16^{INK4A}$ accelerated tumorigenesis in $p53^{-/-}$ mice (40), and similarly, INK4A/ARF knockout mice developed tumors with a shorter latency than $p16^{INK4A-/-}$ or $p19^{ARF-/-}$ mice (41). In a $p16^{INK4A}$ null background, the loss of one $p19^{ARF}$ allele accelerated tumorigenesis, while strikingly, the wild-type allele was retained in a subset of the tumors (25). This indicates that also in vivo, tumor development by abrogation of the pRB pathway can be accelerated by partial ablation of the p53 pathway. Moreover, various mouse tumor models have been generated by combined deletion of *p53* and *Rb*, including tumors of the lung (29), central nervous system (28), breast (42), and pineal and pituitary glands (45). Finally, simultaneous mutations in both pathways have been found in a variety of mouse and human tumor samples (4, 30). Thus, the synergism between the loss of the pocket protein and p53 pathways, as observed in this study during transformation of MEFs, also applies to tumorigenesis in both mice and humans. While this synergism has been explained by alleviation of apoptosis by p53, our previous (11) and present findings indicate that the loss of p53 may also be required for alleviation of cell cycle arrest of cells with abrogated pocket protein function.

Comparison of the requirements for transformation of human and murine fibroblasts. By using variants of simian virus 40 large T antigen (LT) that specifically target p53 or the pRB family, Rangarajan and coworkers (35) suggested that in both human and mouse cells, the loss of p53 or the loss of pocket proteins is sufficient for bypassing Ras^{V12}-induced senescence. However, Ras^{V12}-induced transformation met different requirements in human and murine fibroblasts. First, transformation of human fibroblasts required expression of hTERT and simian virus 40 small t antigen (ST) (16), which was dispensable for transformation of murine fibroblasts. Since murine cells contain long telomeres due to active telomerase (23, 34), mTERT overexpression is not required for transformation. The requirement for ST in transformation of human fibroblasts is caused by its interaction with protein phosphatase 2A (17), which possibly downregulates PTEN (phosphatase and tensin homolog) (3). Why ST expression is not required for murine transformation is currently unknown. Second, LT-mediated ablation of either the pRB or the p53 pathway appeared sufficient for Ras^{V12}-induced transformation of mouse embryonic fibroblasts, while ablation of both pathways was

required for transformation of human fibroblasts (35). Similarly, Boehm et al. (3) claimed that expression of a dominant-negative version of p53, c-Myc, and Ras^{V12} was sufficient for transformation of MEFs, whereas human fibroblasts needed expression of ST and suppression of pRB. Also, Ras^{V12}- and hTERT-expressing BJ primary human fibroblasts could exhibit anchorage-independent growth only upon concomitant knockdown of p53 and pRB (46). Taken together, a widely held view that suppression of both the p53 and pRB pathways is mandatory to transformation of human cells while either one of these events is sufficient for transformation of murine cells has emerged. This view was supported by Sage et al. (38), who reported anchorage-independent growth of TKO MEFs upon expression of Ras^{V12}. However, our previous (7, 32) and present results sharply contrast with this view: partial or complete pocket protein-deficient MEFs were largely unable to exhibit anchorage-independent growth upon Ras^{V12} expression. Furthermore, we found that partial ablation of the p53 pathway strongly stimulated anchorage-independent growth of pocket protein-deficient MEFs. We therefore conclude that in murine cells, ablation of the p53 and pRB pathways synergistically supports oncogenic transformation and that in this respect, mouse fibroblasts are not fundamentally different from human fibroblasts.

ACKNOWLEDGMENTS

We thank George Q. Daley for the pEYK-MCF7 library, Daniel Peeper and Theo van Laar for help with recovery of cDNA vectors, Anja van der Wal for generation of MEFs, Tanja van Harn for kinase assays, Elly Delzenne-Goette and Sjaak Greven for nude mice injections and tumor analyses, Lauran Oomen and Lenny Brocks for help with digital microscopy, and Frank van Diepen and Anita Pfauth for help with FACS. We are grateful to Marieke Aarts, Jan-Hermen Dannenberg, Tanja van Harn, and Rob Wolthuis for helpful discussions and critically reading the manuscript.

This work was financially supported by the Dutch Cancer Society (NKI 2002-2634).

REFERENCES

1. **Bao, W., M. Thullberg, H. Zhang, A. Onischenko, and S. Strömblad.** 2002. Cell attachment to the extracellular matrix induces proteasomal degradation of $p21^{CIP1}$ via Cdc42/Rac1 signaling. Mol. Cell. Biol. **22:**4587–4597.
2. **Berthet, C., and P. Kaldis.** 2007. Cell-specific responses to loss of cyclin-dependent kinases. Oncogene **26:**4469–4477.
3. **Boehm, J. S., M. T. Hession, S. E. Bulmer, and W. C. Hahn.** 2005. Transformation of human and murine fibroblasts without viral oncoproteins. Mol. Cell. Biol. **25:**6464–6474.
4. **Burke, L., D. B. Flieder, D. G. Guinee, E. Brambilla, A. N. Freedman, W. P. Bennett, R. T. Jones, A. Borkowski, N. A. Caporaso, M. Fleming, V. Trastek, P. Pairolero, H. Tazelaar, D. Midthun, J. R. Jett, L. A. Liotta, W. D. Travis, and C. C. Harris.** 2005. Prognostic implications of molecular and immunohistochemical profiles of the Rb and p53 cell cycle regulatory pathways in primary non-small cell lung carcinoma. Clin. Cancer Res. **11:**232–241.
5. **Coats, S., P. Whyte, M. L. Fero, S. Lacy, G. Chung, E. Randel, E. Firpo, and J. M. Roberts.** 1999. A new pathway for mitogen-dependent cdk2 regulation uncovered in $p27^{Kip1}$-deficient cells. Curr. Biol. **9:**163–173.
6. **Dannenberg, J. H., L. Schuijff, M. Dekker, M. van der Valk, and H. te Riele.** 2004. Tissue-specific tumor suppressor activity of retinoblastoma gene homologs p107 and p130. Genes Dev. **18:**2952–2962.
7. **Dannenberg, J. H., A. van Rossum, L. Schuijff, and H. te Riele.** 2000. Ablation of the retinoblastoma gene family deregulates G_1 control causing immortalization and increased cell turnover under growth-restricting conditions. Genes Dev. **14:**3051–3064.
8. **Dirac, A. M., and R. Bernards.** 2003. Reversal of senescence in mouse fibroblasts through lentiviral suppression of p53. J. Biol. Chem. **278:**11731–11734.
9. **Dobrzycka, K. M., K. Kang, S. Jiang, R. Meyer, P. H. Rao, A. V. Lee, and S. Oesterreich.** 2006. Disruption of scaffold attachment factor B1 leads to TBX2 up-regulation, lack of p19ARF induction, lack of senescence, and cell immortalization. Cancer Res. **66:**7859–7863.
10. **Fang, F., G. Orend, N. Watanabe, T. Hunter, and E. Ruoslahti.** 1996. Dependence of cyclin E-CDK2 kinase activity on cell anchorage. Science **271:**499–502.
11. **Foijer, F., R. M. Wolthuis, V. Doodeman, R. H. Medema, and H. te Riele.** 2005. Mitogen requirement for cell cycle progression in the absence of pocket protein activity. Cancer Cell **8:**455–466.
12. **Gad, A., M. Thullberg, J. H. Dannenberg, H. te Riele, and S. Stromblad.** 2004. Retinoblastoma susceptibility gene product (pRb) and p107 functionally separate the requirements for serum and anchorage in the cell cycle G1-phase. J. Biol. Chem. **279:**13640–13644.
13. **Grana, X., J. Garriga, and X. Mayol.** 1998. Role of the retinoblastoma protein family, pRB, p107 and p130 in the negative control of cell growth. Oncogene **17:**3365–3383.
14. **Guadagno, T. M., and R. K. Assoian.** 1991. G1/S control of anchorage-independent growth in the fibroblast cell cycle. J. Cell Biol. **115:**1419–1425.
15. **Guadagno, T. M., M. Ohtsubo, J. M. Roberts, and R. K. Assoian.** 1993. A link between cyclin A expression and adhesion-dependent cell cycle progression. Science **262:**1572–1575.
16. **Hahn, W. C., C. M. Counter, A. S. Lundberg, R. L. Beijersbergen, M. W. Brooks, and R. A. Weinberg.** 1999. Creation of human tumour cells with defined genetic elements. Nature **400:**464–468.
17. **Hahn, W. C., S. K. Dessain, M. W. Brooks, J. E. King, B. Elenbaas, D. M. Sabatini, J. A. DeCaprio, and R. A. Weinberg.** 2002. Enumeration of the simian virus 40 early region elements necessary for human cell transformation. Mol. Cell. Biol. **22:**2111–2123.
18. **Hanahan, D., and R. A. Weinberg.** 2000. The hallmarks of cancer. Cell **100:**57–70.
19. **Harvey, M., A. T. Sands, R. S. Weiss, M. E. Hegi, R. W. Wiseman, P. Pantazis, B. C. Giovanella, M. A. Tainsky, A. Bradley, and L. A. Donehower.** 1993. In vitro growth characteristics of embryo fibroblasts isolated from p53-deficient mice. Oncogene **8:**2457–2467.
20. **Hurford, R. K., Jr., D. Cobrinik, M. H. Lee, and N. Dyson.** 1997. pRB and p107/p130 are required for the regulated expression of different sets of E2F responsive genes. Genes Dev. **11:**1447–1463.
21. **Jacobs, J. J. L., P. Keblusek, E. Robanus-Maandag, P. Kristel, M. Lingbeek, P. M. Nederlof, T. van Welsem, M. J. van de Vijver, E. Y. Koh, G. Q. Daley, and M. van Lohuizen.** 2000. Senescence bypass screen identifies *TBX2*, which represses *Cdkn2a* (*$p19^{ARF}$*) and is amplified in a subset of human breast cancers. Nat. Genet. **26:**291–299.
22. **Kamijo, T., F. Zindy, M. F. Roussel, D. E. Quelle, J. R. Downing, R. A. Ashmun, G. Grosveld, and C. J. Sherr.** 1997. Tumor suppression at the mouse INK4a locus mediated by the alternative reading frame product p19ARF. Cell **91:**649–659.
23. **Kipling, D., and H. J. Cooke.** 1990. Hypervariable ultra-long telomeres in mice. Nature **347:**400–402.
24. **Koh, E. Y., T. Chen, and G. Q. Daley.** 2002. Novel retroviral vectors to facilitate expression screens in mammalian cells. Nucleic Acids Res. **30:**e142.
25. **Krimpenfort, P., K. C. Quon, W. J. Mooi, A. Loonstra, and A. Berns.** 2001. Loss of p16Ink4a confers susceptibility to metastatic melanoma in mice. Nature **413:**83–86.
26. **Lukas, C., C. S. Sorensen, E. Kramer, E. Santoni-Rugiu, C. Lindeneg, J. M. Peters, J. Bartek, and J. Lukas.** 1999. Accumulation of cyclin B1 requires E2F and cyclin-A-dependent rearrangement of the anaphase-promoting complex. Nature **401:**815–818.
27. **Mahlamaki, E. H., M. Barlund, M. Tanner, L. Gorunova, M. Hoglund, R. Karhu, and A. Kallioniemi.** 2002. Frequent amplification of 8q24, 11q, 17q, and 20q-specific genes in pancreatic cancer. Genes Chromosomes Cancer **35:**353–358.
28. **Marino, S., M. Vooijs, G. H. van Der Gulden, J. Jonkers, and A. Berns.** 2000. Induction of medulloblastomas in p53-null mutant mice by somatic inactivation of Rb in the external granular layer cells of the cerebellum. Genes Dev. **14:**994–1004.
29. **Meuwissen, R., S. C. Linn, R. I. Linnoila, J. Zevenhoven, W. J. Mooi, and A. Berns.** 2003. Induction of small cell lung cancer by somatic inactivation of both Trp53 and Rb1 in a conditional mouse model. Cancer Cell **4:**181–189.
30. **Miwa, S., C. Uchida, K. Kitagawa, T. Hattori, T. Oda, H. Sugimura, H. Yasuda, H. Nakamura, K. Chida, and M. Kitagawa.** 2006. Mdm2-mediated pRB downregulation is involved in carcinogenesis in a p53-independent manner. Biochem. Biophys. Res. Commun. **340:**54–61.
31. **Nevins, J. R.** 2001. The Rb/E2F pathway and cancer. Hum. Mol. Genet. **10:**699–703.
32. **Peeper, D. S., J. H. Dannenberg, S. Douma, H. te Riele, and R. Bernards.** 2001. Escape from premature senescence is not sufficient for oncogenic transformation by Ras. Nat. Cell Biol. **3:**198–203.
33. **Prince, S., S. Carreira, K. W. Vance, A. Abrahams, and C. R. Goding.** 2004. Tbx2 directly represses the expression of the $p21^{WAF1}$ cyclin-dependent kinase inhibitor. Cancer Res. **64:**1669–1674.
34. **Prowse, K. R., and C. W. Greider.** 1995. Developmental and tissue-specific regulation of mouse telomerase and telomere length. Proc. Natl. Acad. Sci. USA **92:**4818–4822.
35. **Rangarajan, A., S. J. Hong, A. Gifford, and R. A. Weinberg.** 2004. Species-

and cell type-specific requirements for cellular transformation. Cancer Cell **6:**171–183.

36. **Rodier, G., C. Makris, P. Coulombe, A. Scime, K. Nakayama, K. I. Nakayama, and S. Meloche.** 2005. p107 inhibits G1 to S phase progression by down-regulating expression of the F-box protein Skp2. J. Cell Biol. **168:** 55–66.
37. **Roovers, K., and R. K. Assoian.** 2000. Integrating the MAP kinase signal into the G1 phase cell cycle machinery. Bioessays **22:**818–826.
38. **Sage, J., G. J. Mulligan, L. D. Attardi, A. Miller, S. Chen, B. Williams, E. Theodorou, and T. Jacks.** 2000. Targeted disruption of the three Rb-related genes leads to loss of G_1 control and immortalization. Genes Dev. **14:**3037–3050.
39. **Serrano, M., A. W. Lin, M. E. McCurrach, D. Beach, and S. W. Lowe.** 1997. Oncogenic ras provokes premature cell senescence associated with accumulation of p53 and p16INK4a. Cell **88:**593–602.
40. **Sharpless, N. E., S. Alson, S. Chan, D. P. Silver, D. H. Castrillon, and R. A. DePinho.** 2002. $p16^{INK4a}$ and p53 deficiency cooperate in tumorigenesis. Cancer Res. **62:**2761–2765.
41. **Sharpless, N. E., M. R. Ramsey, P. Balasubramanian, D. H. Castrillon, and R. A. DePinho.** 2004. The differential impact of $p16^{INK4a}$ or $p19^{ARF}$ deficiency on cell growth and tumorigenesis. Oncogene **23:**379–385.
42. **Simin, K., H. Wu, L. Lu, D. Pinkel, D. Albertson, R. D. Cardiff, and D. T. Van Dijke.** 2004. pRb inactivation in mammary cells reveals common mechanisms for tumor initiation and progression in divergent epithelia. PLoS Biol. **2:**E22.
43. **Sinclair, C. S., C. Adem, A. Naderi, C. L. Soderberg, M. Johnson, K. Wu, L. Wadum, V. L. Couch, T. A. Sellers, D. Schaid, J. Slezak, Z. Fredericksen, J. N. Ingle, L. Hartmann, R. B. Jenkins, and F. J. Couch.** 2002. *TBX2* is preferentially amplified in *BRCA1*- and *BRCA2*-related breast tumors. Cancer Res. **62:**3587–3591.
44. **Vance, K. W., S. Carreira, G. Brosch, and C. R. Goding.** 2005. Tbx2 is overexpressed and plays an important role in maintaining proliferation and suppression of senescence in melanomas. Cancer Res. **65:**2260–2268.
45. **Vooijs, M., H. te Riele, M. van der Valk, and A. Berns.** 2002. Tumor formation in mice with somatic inactivation of the retinoblastoma gene in interphotoreceptor retinol binding protein-expressing cells. Oncogene **21:**4635–4645.
46. **Voorhoeve, P. M., and R. Agami.** 2003. The tumor-suppressive functions of the human INK4A locus. Cancer Cell **4:**311–319.
47. **Walker, J. L., A. K. Fournier, and R. K. Assoian.** 2005. Regulation of growth factor signaling and cell cycle progression by cell adhesion and adhesion-dependent changes in cellular tension. Cytokine Growth Factor Rev. **16:**395–405.
48. **Williams, J. P., T. Stewart, B. Li, R. Mulloy, D. Dimova, and M. Classon.** 2006. The retinoblastoma protein is required for Ras-induced oncogenic transformation. Mol. Cell. Biol. **26:**1170–1182.
49. **Wu, R. C., and A. H. Schonthal.** 1997. Activation of p53-p21waf1 pathway in response to disruption of cell-matrix interactions. J. Biol. Chem. **272:**29091–29098.
50. **Zhu, X., M. Ohtsubo, R. M. Bohmer, J. M. Roberts, and R. K. Assoian.** 1996. Adhesion-dependent cell cycle progression linked to the expression of cyclin D1, activation of cyclin E-cdk2, and phosphorylation of the retinoblastoma protein. J. Cell Biol. **133:**391–403.